arXiv:0912.3793v1 [cond-mat.other] 18 Dec 2009

# Formation of a mesa shaped phonon pulse in superfluid $^4$He

I.N. Adamenko, K.E. Nemchenko, and V.A. Slipko
V.N. Karazin Kharkov National University, 61077, Ukraine

December 18, 2009

E-mail: valery.slipko@gmail.com

**Abstract**

We present a theory for the formation of a mesa shaped phonon pulse in superfluid $^4$He. Starting from the hydrodynamic equations of superfluid helium, we obtain the system of equations which describe the evolution of strongly anisotropic phonon systems. Such systems can be created experimentally. The solution of the equations are simple waves, which correspond to second sound in the moving phonon pulse. Using these exact solutions, we describe the expansion of phonon pulses in superfluid helium at zero temperature. This theory gives an explanation for the mesa shape observed in the measured phonon angular distributions. Almost all dependencies of the mesa shape on the system parameters can be qualitatively understood.

## 1 Introduction

It is at present, impossible to create in superfluid helium, a constant relative velocity, **w**, between the normal and superfluid which is close to the Landau critical velocity. However phonon pulses can be created, which are pulses of normal fluid moving through the stationary superfluid with a high relative velocity, without superfluidity breaking down [1, 2, 3, 4, 5]. These pulses are $t_p = 10^{-5} - 10^{-7}$s, long.

In experiments [1]-[5] a heater is immersed in superfluid helium at ∼50 mK. A current pulse, applied to the heater, creates a moving phonon system in the stationary superfluid. The initial transverse and longitudinal dimensions of such a phonon system is determined by the heater size and the duration of the current pulse respectively. Then the phonon system starts to expand as it moves in the superfluid helium. There are two very different regimes of such evolution. At pressure above 19 bar phonons propagate almost without scattering. So there is ballistic propagation. In this case, the phonon energy has an angular distribution with a characteristic cosine dependence. At lower pressures, the phonons strongly interact by three phonon processes. These are prohibited by the phonon energy-momentum conservation laws at pressure above 19 bar. Therefore at low pressures there can be a hydrodynamic regime, when phonon system expands in "phonon vacuum" in a way similar to the ordinary expansion of a gas into a vacuum.

In a recent paper [5] detailed measurements of the angular distributions of the energy in the phonon pulse were reported at zero pressure. The measurements were made at different distances from the heater, with various heater sizes and heater powers. The results showed a notable feature; the angular dependence of the energy flux has a flat top, and concave steep sides. In [5] this kind of distribution was called a mesa shape. Such a phonon energy distributions cannot occur in the ballistic regime. In this case we would have cosine-like convex angular distribution, as it follows both from experiments at high enough pressure and from theoretical considerations (Lambert's law). At zero pressure we have, despite the assumptions made in the theoretical model in [5], a hydrodynamic regime due to three phonon processes in the wings of the angular distribution, where the phonon density is sufficiently high, as well as in the centre of the pulse. The dependencies of the mesa width and height on various parameters, obtained in [5], are nontrivial. So the hydrodynamic propagation of phonon systems in superfluid helium is an important problem.

To choose a method of theoretically analysing the phonon pulse expansion in superfluid helium, we should take into account that in experiments [2, 3, 4, 5] the phonon pulse duration is much greater than the time to attain a local equilibrium. Therefore there is a dynamic equilibrium which arises mainly due to scattering by three phonon processes, which have a characteristic time $t_{3pp} \sim 10^{-8}$s [6]. This applies to the experimental conditions [2, 3, 4, 5]. Fast relaxation has been observed directly in the experiments with colliding phonon pulses [7]. There is further evidence from the fact that a phonon pulse propagates in superfluid helium as a whole, with a velocity which is experimentally indistinguishable from the Landau critical velocity for phonons. For phonons with a linear energy-momentum relation, $\varepsilon(p) = cp$, the Landau critical velocity is equal to $c$ [8].

Thus the strong three-phonon scattering, within a pulse comprised of low energy phonons in liquid helium at 0 bar, leads to a quasi equilibrium. The equilibrium state of the phonons can be defined in terms of a temperature and a drift velocity, which means we can use a hydrodynamic approach to describe the dynamics of the phonon pulse.

Another feature of such phonon systems is that the energy density in the phonon pulse is much larger than the ambient phonon energy density in superfluid helium. Therefore the evolution of a strongly anisotropic phonon system is essentially nonlinear. Nonlinear waves in superfluid helium, when $w$ is small, have been studied for many years, but the analysis of nonlinear waves at arbitrary $w$ has not been done until now. The first such analysis was made in Ref. [9], where the phonon pulse evolution were studied by using the Bose-cone model for the phonon distribution function. There, the nonlinear equations of gas-dynamic type for the parameters of the Bose-cone model were obtained. These equations were solved for one dimensional transverse and longitudinal evolution of a phonon pulse. In [10] and [11] the more reasonable Bose-Einstein phonon distribution function was used instead of the Bose-cone distribution. But the approximate theories developed in these papers only allowed us to study phonon evolution which was near to the initial state (see [11]). The question of the mesa shaped angular distribution did not even occur in [10] and [11], because this phenomenon was only fully investigated recently [5].

In the present paper we rigorously solve the problem of phonon pulse expansion into the "superfluid vacuum" of helium. This gives a physical explanation of the mesa shape formation and the nontrivial dependencies of the mesa width and height on various parameters.

In Sec. II we obtain the nonlinear equations, which describes the evolution of phonon systems created by thermal pulses in superfluid helium. In Sec. III we find explicitly the family of exact solutions of these equations. They are the simple waves, which correspond to the second sound modes in phonon systems. In Sec. IV these exact solutions are used to describe the first stage of the expansion of a phonon layer in superfluid helium, when only the incident waves exist. Here we find the expansion velocity of a phonon pulse into the "phonon vacuum", i.e. into superfluid helium with zero temperature. The second stage of the expansion of the phonon layer, when reflected waves are formed, are studied in Sec. V. Here we develop an approximate method to describe the reflected wave, which allows us to find the average energy density and the width of the reflected wave. In Sec. VI by using the theory presented in this paper we give qualitative explanations of some experimental data from Ref. ([5]). Conclusions are drawn in Sec. VII.

# 2 Equations for the evolution of a phonon system in the hydrodynamic approximation

To describe the evolution of a phonon system in superfluid helium, we start from the well-known two-fluid hydrodynamic equations in the non-dissipative approximation [12, 13]:

$$\frac{\partial\rho}{\partial t} + div(\rho_n \mathbf{v}_n + \rho_s \mathbf{v}_s) = 0; \tag{1}$$

$$\frac{\partial S}{\partial t} + div(S\mathbf{v}_n) = 0; \tag{2}$$

$$\frac{\partial \mathbf{v}_s}{\partial t} + \nabla\mu + (\mathbf{v}_s\nabla)\mathbf{v}_s = 0; \tag{3}$$

$$\frac{\partial A_i}{\partial t} + (\mathbf{v}_n\nabla)A_i = -\frac{\partial T}{\partial x_i} - A_k\frac{\partial v_{nk}}{\partial x_i}. \tag{4}$$

Here $\rho$ is the density of helium; $\rho_n$ and $\rho_s$ are densities of the normal and superfluid components respectively; $\mathbf{v_n}$ and $\mathbf{v_s}$ are velocities of normal and superfluid components respectively; $S$ is the entropy of unit of volume; $\mu$ is the chemical potential of unit of mass of helium; $\mathbf{A} = \rho_n\mathbf{w}/S$; $\mathbf{w} = \mathbf{v}_n - \mathbf{v}_s$ is the relative velocity of the normal and superfluid components; $T$ is temperature. Summation over twice repeated indices $k$ is implied in Eq. (4). Eqs. (1) and (2) express the conservation of mass and entropy respectively, Eq. (3) expresses the acceleration of the superfluid and Eq. (4) is a combination of momentum conservation and other conservation laws.

In the experiments of Refs. [1]-[5], phonon systems were created by a heater immersed in superfluid helium. The temperature of the liquid helium was $\sim 50$ mK. At this temperature, the ambient thermal excitations can be neglected. The power of the applied heat pulses was such that the normal density $\rho_n$ was very small, $\rho_n \ll \rho$. In this case the superfluid velocity and variations of pressure can be neglected when we study phonon propagation [14]. Taking into account the approximate relation $\mathbf{v}_n = \mathbf{w} + \mathbf{v}_s \approx \mathbf{w}$ in Eqs. (2) and (4), we obtain the system of equations which describes the evolution of a phonon system:

$$\frac{\partial S}{\partial t} + div(S\mathbf{w}) = 0; \tag{5}$$

$$\left(\frac{\partial}{\partial t} + (\mathbf{w}\nabla)\right)\left(\frac{\rho_n}{S}\mathbf{w}\right) = -\nabla T - \frac{\rho_n}{2S}\nabla w^2. \tag{6}$$

Relations (5) and (6) are the system of four equations for four variables, for example, for temperature $T$ and the components of relative velocity $\mathbf{w}$. Eqs. (5) and (6) must be completed by the equations of state of superfluid helium $S = S(T, w^2)$, $\rho_n = \rho_n(T, w^2)$, in which we have neglected the pressure dependence in accordance with the assumptions made above.

The system of Eqs. (5)-(6) are linearized for small deviations of the variables. They define the propagation of second sound waves and the transverse wave, at arbitrary values of the equilibrium relative velocity $w$, when $\rho_n \ll \rho$. The dispersion relation for this case is studied in [14].

For a phonon system with a linear energy-momentum relation $\varepsilon = cp$, where $c^2 = (\partial P)/(\partial \rho)$ and $c$ is the first sound velocity of helium, we have [12]:

$$\frac{\rho_n}{S} = \frac{T}{c^2 - w^2}, \quad S = \frac{2\pi^2}{45} \frac{k_B^4 T^3}{\hbar^3 c^3 (1 - w^2/c^2)^2}. \tag{7}$$

The system of equations (5)-(6), together with the relations (7), describe the evolution of phonon systems propagating in superfluid helium.

The main feature of phonon systems, created in experiments [1]-[5], is the high value of the relative velocity $w$, which has a value close to the first sound velocity $c$. At the same time the temperature of such phonon systems is very small, so the normal density satisfies the strong inequality $\rho_n \ll \rho$. As shown in [15], using the general conditions of stability for superfluid helium [8], such phonon systems are thermodynamically stable, even for values of the relative velocity which approach the first sound velocity $c$, if the temperature is low enough.

In a recent paper [5] detailed measurements of angular distributions of energy in phonon systems were reported for different distances from the heater, and different heater sizes and powers. Fig.1 illustrates the main idea of the experiments [5]. The phonon system (shaded region) is created by a current pulse in the heater H, which is immersed in superfluid helium.

The created phonon system moves in the direction normal to the heater (axis $z$) with a velocity close to the first sound velocity $c$. The pulse expands transversely. This expansion along with the initial phonon energy distribution near the heater, determines the angular distribution of energy on the detector. By changing the heater size, one can vary the initial transverse size $L_0$ of the phonon system, and by the changing heater pulse duration $t_p$ one can vary the characteristic length $ct_p$ of the system.

We consider the simple case when the dependence on $z$ can be neglected in the initial value problem for Eqs. (5), (6). That is valid for sufficiently long phonon pulses. To study the behaviour of the transverse expansion of phonon pulses, we consider the 2 dimensional case, where all values depend

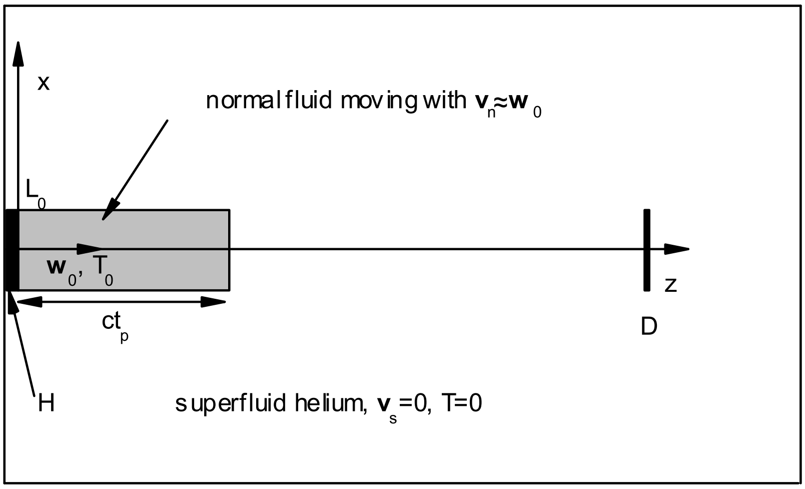
x
normal fluid moving with $\mathbf{v}_n \approx \mathbf{w}_0$
$L_0$
$\mathbf{w}_0$, $T_0$
$ct_p$
z
D
H
superfluid helium, $\mathbf{v}_s$=0, T=0

Figure 1: A phonon system (shaded region) with characteristic temperature $T_0$ and the relative velocity $\mathbf{w}_0$ in superfluid helium with $\mathbf{v}_s = 0$ and temperature $T = 0$. The heater H has a width $2L_0$. The characteristic length $ct_p$ of the system depends on the the pulse duration $t_p$. The coordinate frame is defined with the $z$-axis parallel to the normal to the heater H. D is the detector.

only on one spatial cartesian coordinate, $x$. The relative velocity $\mathbf{w}$ lies in the plane $xz$, i.e. $\mathbf{w} = (w_x, 0, w_z)$.

Substituting Eqs. (7) into Eqs. (5), (6), and introducing the dimensionless variables

$$\Theta = \ln \frac{T}{1-u^2}, \quad u_x = w_x/c, \quad u^2 = (w_x^2 + w_z^2)/c^2, \tag{8}$$

we can rewrite the equations in the matrix form

$$\frac{\partial}{c\partial t} \begin{pmatrix} \Theta \\ u_x \\ u^2 \end{pmatrix} + M(u_x, u^2) \frac{\partial}{\partial x} \begin{pmatrix} \Theta \\ u_x \\ u^2 \end{pmatrix} = 0, \tag{9}$$

where the matrix $M(u_x, u^2)$ is equal to

$$\frac{1}{3-u^2} \begin{pmatrix} (5-3u^2)u_x & 1-u^2 & -u_x \\ (1-u^2)(3-u^2-2u_x^2) & 2u_x & -0.5(3-u^2-2u_x^2) \\ 6(1-u^2)^2 u_x & -2u^2(1-u^2) & 2u^2 u_x \end{pmatrix}. \tag{10}$$

We have introduced the dimensionless relative velocity $\mathbf{u} = \mathbf{w}/c$ in Eqs. (8)-(10).

We see that Eqs. (9)-(10) is a complicated nonlinear system of first order equations in partial derivatives, with coefficients that depend explicitly on the variable $u^2$ and linearly and quadratically on the variable $u_x$. We show below that Eqs. (9)-(10) can be solved exactly for arbitrary values of the relative velocity $w$.

# 3 Second sound simple waves in phonon systems

In this section we will obtain the class of exact solutions for the system of Eqs. (9)-(10). In Sec. 4 we apply the solutions, along with the initial conditions, to the problem of phonon pulse expansion in superfluid helium with zero temperature.

Let us suppose that all three variables of the system of Eqs. (9)-(10) depend on one unknown function, for example, $\nu = \nu(x,t)$. In other words we seek solution in the form of $\Theta = \Theta(\nu)$, $u_x = u_x(\nu)$, and $u^2 = u^2(\nu)$. Such solutions are called simple waves (see, for example, [16]). Substituting these relations into equations (9), and dividing the equations (9) by $\partial\nu/\partial x$ we obtain the following matrix equation

$$M\frac{d}{d\nu}\begin{pmatrix}\Theta\\ u_x\\ u^2\end{pmatrix} = -\frac{\frac{\partial\nu}{c\partial t}}{\frac{\partial\nu}{\partial x}}\frac{d}{d\nu}\begin{pmatrix}\Theta\\ u_x\\ u^2\end{pmatrix}. \tag{11}$$

We see from Eq. (11) that the vector with components $(d\Theta/d\nu, du_x/d\nu, du^2/d\nu)$ is an eigenvector of the matrix $M$, which corresponds to the eigenvalue $-\frac{\partial\nu}{c\partial t}/\frac{\partial\nu}{\partial x}$. Thus, if we know some eigenvector $r = (r_1, r_2, r_3)$ of the matrix $M$ (10), which corresponds to the eigenvalue $\tilde{V}$, i.e. if $\sum_{k=1}^{3} M_{ik}r_k = \tilde{V}r_i$ for any index $i \in (1,2,3)$, then from Eq. (11) we obtain the running wave equation for the function $\nu(x,t)$

$$\frac{\partial\nu(x,t)}{c\partial t} + \tilde{V}(\nu)\frac{\partial\nu(x,t)}{\partial x} = 0, \tag{12}$$

which has velocity $c\tilde{V}$. The system of ordinary differential equations for this solution is

$$\frac{d\Theta}{d\nu} = \lambda r_1, \quad \frac{du_x}{d\nu} = \lambda r_2, \quad \frac{du^2}{d\nu} = \lambda r_3, \tag{13}$$

where $\lambda$ is some multiplier. Below we will show that matrix $M$ (10) has three pairwise different eigenvalues. Therefore the eigenvectors, which correspond to the same eigenvalue, are collinear, and $\lambda$ is a coefficient of proportionality between a given eigenvector $r = (r_1, r_2, r_3)$ and the eigenvector with components $(d\Theta/d\nu, du_x/d\nu, du^2/d\nu)$.

Eliminating $\lambda$ from the system (13), we get the system of ordinary differential equations

$$\frac{d\Theta}{r_1} = \frac{du_x}{r_2} = \frac{du^2}{r_3}, \tag{14}$$

where $r = (r_1, r_2, r_3)$ is a eigenvector of matrix (10) of system (9), which corresponds to the eigenvalue $\tilde{V}$. The equations (14) determine the functional dependence between the variables $\Theta$, $u_x$, and $u^2$ in the corresponding simple wave solution of system (9), (10). It follows from Eqs. (12) and (13), that any of the variables $\Theta$, $u_x$, and $u^2$ satisfy the same running wave equation (12) as the function $\nu(x,t)$.

The three eigenvalues of matrix (10) are calculated to be

$$\tilde{V}_1 = \frac{2u_x - \sqrt{(1-u^2)(3-u^2-2u_x^2)}}{3-u^2}, \tag{15}$$

$$\tilde{V}_2 = \frac{2u_x + \sqrt{(1-u^2)(3-u^2-2u_x^2)}}{3-u^2}, \tag{16}$$

$$\tilde{V}_3 = u_x. \tag{17}$$

It should be noted that the eigenvalues (15)-(17) of matrix (10) of system of Eqs. (9) are real, if $u < 1$, and $\tilde{V}_1 < \tilde{V}_3 < \tilde{V}_2$. Thus the system of Eqs. (9) are hyperbolic. In this connection it is interesting to note, that the condition $w < c$, which guaranties hyperbolicity of the system of Eqs. (9), (10) coincides here with the condition of thermodynamic stability for a phonon system [15].

The expressions (15)-(17) give the simple wave velocities $V_{1,2,3} = c\tilde{V}_{1,2,3}$ in a phonon system. Two of these velocities coincide, as they should, with those of second sound propagation in a phonon system [14] and the third with the velocity of transverse waves [17]. In this case, the values $u_x$ and $u^2$ in Eqs. (15)-(17) are the mean constant equilibrium values, from which there are small perturbations of temperature and relative velocity, which propagate with velocities (15)-(17). Velocities (15) and (16) correspond to the second sound propagation velocities, which were found in [14] for arbitrary values of relative velocity $w$. Particularly, at $w = 0$, we obtain $V_{1,2} = \mp c/\sqrt{3}$ which is the well-known phonon second sound velocity, when $\rho_n \ll \rho$. Specific features of second sound in anisotropic phonon systems with $w \neq 0$, i.e. when the system is characterised by a certain direction of the relative velocity $\mathbf{w}$, were studied in [14].

The simple wave velocity (17) corresponds to the one for the so-called transverse wave with the dispersion law $\omega = \mathbf{k}\mathbf{v_n} \approx \mathbf{k}\mathbf{w} = k w_x$. The properties of the transverse wave and possibility of realising it in phonon pulses, were discussed in [17].

Let us consider the simple second sound wave with velocity (15). The corresponding eigenvector of matrix (10) is equal to

$$r = \begin{pmatrix} r_1 \\ r_2 \\ r_3 \end{pmatrix} = \begin{pmatrix} 2u_x - (1-u^2)R \\ (1-u^2)(u_x+R)R \\ 2(1-u^2)(3u_x+u^2R) \end{pmatrix}, \tag{18}$$

where we denote

$$R = \sqrt{\frac{3-u^2-2u_x^2}{1-u^2}}. \tag{19}$$

Substituting the second and third components of the eigenvector (18) into the system of equations (14), we obtain the equation

$$\frac{du_x}{R(u_x+R)} = \frac{du^2}{2(3u_x+u^2R)}, \tag{20}$$

which determines the functional connection between $u_x$ and $u^2$ in the simple second sound wave with the velocity $\tilde{V}_1$ (15).

Eqs. (20) can be integrated by changing variable $u^2$ to variable $R$ (19). After this substitution we get the differential equation with separated variables

$$\frac{du_x}{1-u_x^2} = \frac{2R^2dR}{(R^2-3)(R^2-1)}, \tag{21}$$

which can be immediately integrated. Its solution is

$$u_x(R) = \frac{\lambda-1}{\lambda+1}, \quad \lambda = C_1\left(\frac{R-\sqrt{3}}{R+\sqrt{3}}\right)^{\sqrt{3}}\left(\frac{R+1}{R-1}\right), \tag{22}$$

where $C_1$ is an integration constant.

Solving Eq. (19) with respect to $u^2$, we find

$$u^2(R) = 1 - 2\frac{(1-u_x^2)}{R^2-1}. \tag{23}$$

Relations (22) and (23) give, in parametric form, the functional connection between the $x$-component $u_x$, of the dimensionless relative velocity $\mathbf{u}$, and its square $u^2$, which corresponds to velocity $\tilde{V}_1$, in the simple second sound wave (15).

Substituting the first and second component of the eigenvector (18) into the system of equations (14), we obtain the other equation

$$d\Theta = \frac{(2u_x - (1-u^2)R)du_x}{(1-u^2)(u_x+R)R}. \tag{24}$$

Expressing $u^2$ in terms of $R$, and $u_x$ by using Eq. (23) in the factor outside $du_x$ in Eq. (24), we get the following equation instead of Eq. (24)

$$d\Theta - \frac{u_x du_x}{1-u_x^2} = -\frac{du_x}{R(1-u_x^2)}. \tag{25}$$

Now, using Eq. (21) in the right-hand side of Eq. (25), we again get a differential equation with separated variables. By integrating this equation, and then, taking into account the definition (8) of variable $\Theta$, we obtain an expression for the temperature $T$ in the simple second sound wave

$$T(R) = C_2\sqrt{\frac{(1-u_x^2)}{(R^2-3)(R^2-1)}}, \tag{26}$$

where $C_2$ is an integration constant.

Thus the relations (22), (23), and (26) express in parametric form the relationships between the $x$-component $u_x$ of the dimensionless relative velocity $\mathbf{u}$, the square of the dimensionless relative velocity $u^2$, and temperature $T$, in the simple second sound wave, which propagates in "superfluid vacuum" of $^4$He with the velocity $\tilde{V}_1$ (15). The expression for the velocity $\tilde{V}_1$ (15) can be transformed into a more simple form using (23)

$$\tilde{V}_1(R) = \frac{Ru_x - 1}{R - u_x}. \tag{27}$$

It follows from Eqs. (21), (23), and (26), that $u_x$ and $u^2$ increase monotonically when $R$ increases, and $T$ decreases monotonically when $R$ increases. Thus starting from any of the variables $u_x$, $u^2$, or $T$ at the initial moment of time we can determine the corresponding initial function $R(x, t=0)$. The time evolution of the value of $R$ is determined by the running wave equation:

$$\frac{\partial R(x,t)}{c\partial t} + \tilde{V}_1(R)\frac{\partial R(x,t)}{\partial x} = 0, \tag{28}$$

where $\tilde{V}_1(R)$ is the velocity (27). The solution of Eq. (28) is well-known

$$x - c\tilde{V}_1(R)t = f(R), \tag{29}$$

where $f(R)$ is an arbitrary function.

The solution (29) shows that every value of $R$ runs with its own velocity $V_1(R)$ in the simple second sound wave. The relations (29),(27) along with the expressions (22), (23), and (26), express in parametric form the spatial dependence of the $x$-component $w_x = cu_x$ of the relative velocity $\mathbf{w}$, the square of the relative velocity $w^2 = c^2u^2$, and temperature $T$ in the simple second sound wave at any moment of time.

It follows from Eq. (27), that $dV_1(R)/dR > 0$. So it is clear that a simple second sound wave can, in general, give rise to a break in the continuous solution . To determine the location and the velocity of the break we should return to the energy and momentum conservation laws, however we will not be concerned with that problem here.

The other simple second sound wave, which has the velocity $V_2$ (see Eq. (16)), can be obtained from the solution (22), (23), and (26), which corresponds to the velocity $V_1$. For this purpose let us note that if $T(x,t)$, $w_x(x,t)$ and $w^2(x,t)$ is a solution of the system (8)-(10), then $T(-x,t)$, $-w_x(-x,t)$ and $w^2(-x,t)$ is also a solution. This transformation maps one simple second sound wave to the other.

## 4 Expansion of a phonon pulse into the "phonon vacuum" of superfluid helium

To study the main features of the transverse expansion of phonon pulses in superfluid helium we will solve the following problem. Let superfluid helium with $\mathbf{v}_s = 0$ fill up all space. Let us consider the initial conditions

$$T(x,0) = \begin{cases} T_0, |x| < L_0 \\ 0, |x| > L_0 \end{cases} ; \quad w_x(x,0) = 0; \quad w^2(x,0) = w_0^2, \tag{30}$$

for the system of Eqs. (8), (9) and (10).

At the initial time $t = 0$, in the superfluid helium at $T = 0$, there is a layer of phonons of width $2L_0$, temperature $T = T_0$, and relative velocity $\mathbf{w} = (0, 0, w_0)$ directed along $z$-axis (see Fig.2). The phonons in this initial layer is the normal fluid, and as the phonon density is very low the normal fluid density is very small so $\rho_n \ll \rho$. Therefore we can neglect the superfluid velocity and pressure changes when we study the development of the phonon system. Thus the set of Eqs. (9) and (10) apply to this phonon system. We are interested in finding the development in time of the temperature $T$ and the relative velocity $\mathbf{w}$ of the phonon system.

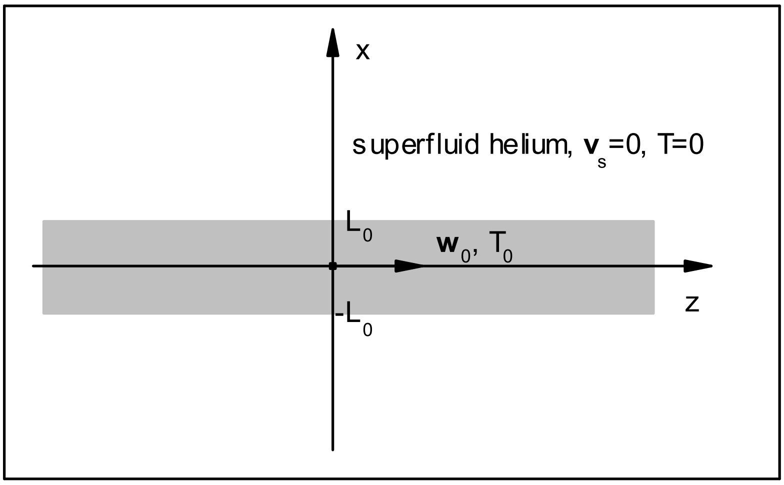

Figure 2: A layer of phonons with temperature $T_0$ and the relative velocity $\mathbf{w}_0 = w_0\mathbf{e}_z$ in superfluid helium with $\mathbf{v}_s = 0$ and temperature $T = 0$. The layer width is $2L_0$. The $x$-axis is directed perpendicularly to the plane of the layer.

The problem, formulated above, can be solved partly by using the simple second sound wave solution found in the previous section. First of all we note that the initial conditions (30) satisfy the symmetry transformations discussed at the end of section 3. Therefore at any time, the temperature $T$ and $w^2$ are even functions of the $x$-coordinate, and $w_x$ is an odd function. Below we will only discuss the solution for domain $x > 0$.

The strong discontinuity, which exists at $x = L_0$ in the initial conditions, disappears immediately after $t = 0$, as it is clear from physical considerations. The phonon gas expands into the superfluid helium with zero temperature, forming the forward front of the outgoing second sound wave (see Fig.3). At the same time, the initial perturbation, in the form of a weak discontinuity, moves in the region $x < L_0$ forming the rear front of the ingoing second sound wave (see Fig.3). The weak discontinuity is at the point where the temperature starts to change from its initial value (30), and it moves towards the coordinate origin $x = 0$ with the velocity $c\tilde{V}_1(u_x = 0, u_0^2 = w_0^2/c^2)$ determined by Eq. (15). Thus until the time $t_0$ when the intersection point reaches $x = 0$, there is no length scale in the problem, and the solution must be self-similar. The value of $t_0$ is given by

$$t_0 = \frac{L_0}{|V_1(u_x = 0, u_0^2 = w_0^2/c^2)|} = \frac{L_0}{c}\sqrt{\frac{3 - w_0^2}{1 - w_0^2}}, \tag{31}$$

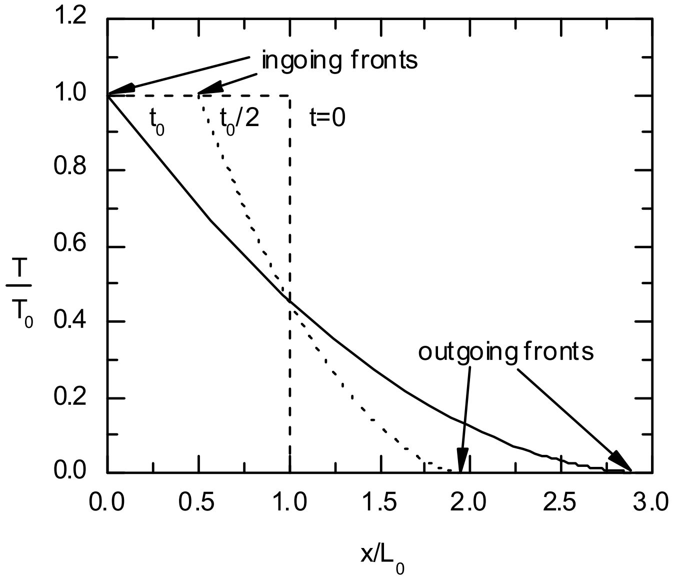

Figure 3: The dependence of the temperature $T$ on the x-coordinate for the initial value $w_0 = 0.95c$ at time $t = 0$ (dashed line), $t = t_0/2$ (dotted line), and $t = t_0$ (solid line). The arrows point to the location of the fronts of the ingoing and outgoing waves at times $t = t_0/2$ and $t = t_0$.

A self-similar solution is a particular case of a simple wave. Therefore from Eq. (29), taking into account that at the initial time $t = 0$ the wavefront is at $x = L_0$, we get $f(R) = L_0$. Thus the function $f(R)$ is reduced to constant for the self-similar solution and

$$x = L_0 + V_1(R)t \tag{32}$$

where $V_1(R) = c\tilde{V}_1(R)$ is determined by the relation (27).

For any moment of time $0 < t < t_0$, the wave occupies the domain $x \in (x_{in}(t), x_{out}(t))$, where value $x_{in}(t) = L_0 + V_1(R_0)t$ determines the position of the front of the ingoing wave, and $x_{out}(t) = L_0 + V_1(R_{out})t$ determines the position of the front of the outgoing wave, which follows from Eq. (32) (see Fig.3). We denote the yet-unknown limits of the variable $R$ as $R_0$ and $R_{out}$, i.e. $R \in (R_0, R_{out})$. Below we show that $R_{out} = +\infty$, and that the value $R_0$ is determined by Eq. (35) coinciding with the value $R(u_x = 0, u_0^2 = w_0^2/c^2)$ from Eq. (19).

To determine the integration constants, which are contained in Eqs. (22) and (26), we should join continuously the simple wave solution (22), (23) and (26) with the to the initial values (30) at $R = R_0$ at the front of the ingoing wave. Thus we get the solution

$$u_x(R) = \frac{\lambda - 1}{\lambda + 1},\ \lambda = \left(\frac{R_0 - 1}{R_0 + 1}\right)\left(\frac{R_0 + \sqrt{3}}{R_0 - \sqrt{3}}\right)^{\sqrt{3}}\left(\frac{R + 1}{R - 1}\right)\left(\frac{R - \sqrt{3}}{R + \sqrt{3}}\right)^{\sqrt{3}}, \tag{33}$$

$$T(R) = T_0\sqrt{\frac{(R_0^2 - 3)(R_0^2 - 1)}{(R^2 - 3)(R^2 - 1)}(1 - u_x^2)}, \tag{34}$$

and the value $R_0$

$$R_0 = \sqrt{\frac{3 - w_0^2/c^2}{1 - w_0^2/c^2}}. \tag{35}$$

On the front of the outgoing wave, in accordance with the initial conditions (30) the phonon temperature is equal to zero. It follows from Eqs. (34) and (33) that this can only be satisfied by $R_{out} = +\infty$.

Thus for any $t \in (0, t_0)$, Eqs. (33), (34), (23), (32), and (27) determine the desired self-similar solution of the initial value problem (9), (10), and (30), and give the values of $T$, $w_x = cu_x$, and $w^2 = c^2u^2$ at any point $x \in (x_{in}(t), x_{out}(t))$.

From Eq. (33) we find that at the front of the outgoing wave, which borders with superfluid helium at zero temperature, the $x$-component of the dimensionless relative velocity $u_x$ is equal to

$$u_{xout} = u_x(R = +\infty) = \frac{\lambda_{out} - 1}{\lambda_{out} + 1},\ \lambda_{out} = \left(\frac{R_0 - 1}{R_0 + 1}\right)\left(\frac{R_0 + \sqrt{3}}{R_0 - \sqrt{3}}\right)^{\sqrt{3}}. \tag{36}$$

From Eq. (27) it follows that this velocity $w_{xout}$ coincides with the velocity of the front of the outgoing wave

$$V_1(R_{out} = +\infty) = w_{xout} = cu_{xout}. \tag{37}$$

Also from Eq. (27) in accordance with Eq. (31) for the velocity of the front of the ingoing wave, we get

$$V_1(R_0) = -\frac{c}{R_0} = -c\sqrt{\frac{1 - w_0^2}{3 - w_0^2}}, \tag{38}$$

which coincides with the velocity $c\tilde{V_1}(u_x = 0, u_0^2 = w_0^2/c^2)$ determined by Eq. (15).

It is interesting that the relative velocity at the front of the outgoing wave, which follows from Eq. (23), is equal to the phonon velocity i.e. $w^2(R_{out} =$

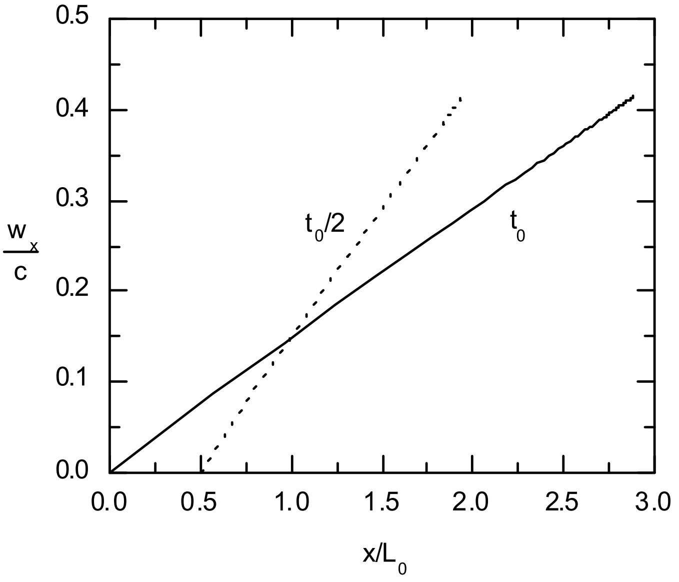

Figure 4: The dependence of $x$-component $w_x$ of the relative velocity on the x-coordinate, for the initial value $w_0 = 0.95c$ for times $t = t_0/2$ (dotted line), and $t = t_0$ (solid line).

$+\infty) = c^2$. Whereas the temperature of such phonons is equal to zero. Therefore such phonon system remains thermodynamically stable [15]. The phonon energy density at the front of the outgoing wave tends to zero.

Figs.3, 4, 5 show the spatial dependence of the temperature $T$ (Fig.3 ), the $x$-component $w_x$ (Fig.4) of the relative velocity $\mathbf{w}$, and the square of the relative velocity $w^2$ (Fig.5) for times $t = 0$ (dashed lines on Figs.3 and 5), $t = t_0/2$ (dotted lines in Figs.3, 4, and 5), and for $t = t_0$ (solid lines in Figs.3, 4, and 5). These graphs are calculated from Eqs. (33), (34), (23), (32), and (27) taking into account (35) for the initial value $w_0 = 0.95c$, which corresponds to a strongly anisotropic phonon system. We see that temperature (Fig.3) of the phonon pulse, expanding in "phonon vacuum", decreases monotonically, but the $x$-component $w_x$ (Fig.4) of the relative velocity $\mathbf{w}$, and the square of the relative velocity $w^2$ (Fig.5) increase when $x$-coordinate increases.

Let us find all the variables at the point $x = L_0$. If we substitute $x = L_0$ in Eq. (32), then we get the equation $V_1(R^*) = 0$, where we denote as $R^*$ the value of $R$, which corresponds to $x = L_0$ at any time $t > 0$. Taking into account Eq. (27), we obtain the equivalent equation $R^* u_x(R^*) = 1$. Solving

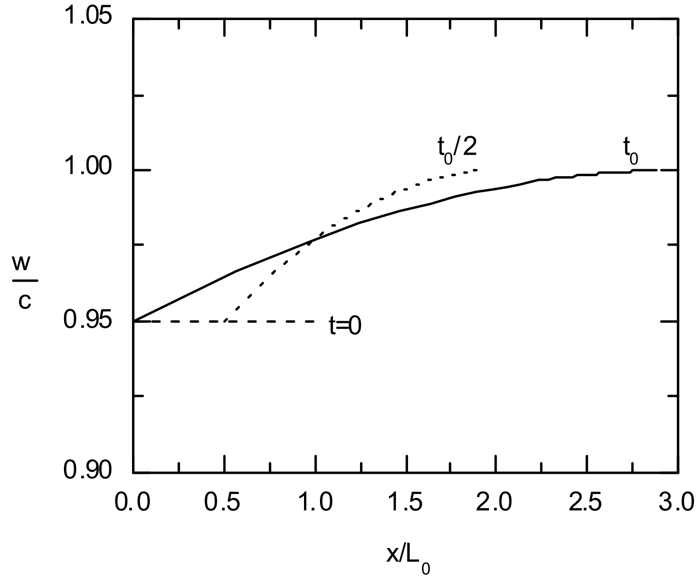

Figure 5: The dependence of the absolute value of the relative velocity $w$ on the x-coordinate for the initial value $w_0 = 0.95c$ for times $t = 0$ (dashed line), $t = t_0/2$ (dotted line), and $t = t_0$ (solid line).

this equation taking into account the expression (33), we get

$$R^* = \sqrt{3}\frac{1+\gamma}{1-\gamma}, \ \gamma = \left(\frac{R_0 - \sqrt{3}}{R_0 + \sqrt{3}}\right)\left(\frac{R_0+1}{R_0-1}\right)^{\frac{1}{\sqrt{3}}}, \tag{39}$$

where $R_0$ is determined by Eq. (35).

Substituting the value $R^*$, determined by (39), into Eqs. (33), (34), and (23), we obtain the temperature $T(R^*)$, the $x$-component $w_x(R^*)$ of the relative velocity $\mathbf{w}$, and the square of the relative velocity $w^2(R^*)$ at $x = L_0$, i.e. these are the values at the initial pulse boundary, for any time while the solution is self-similar. In particular we get

$$u_x(R^*) = \frac{1}{R^*}, \ \ u^2(R^*) = 1 - \frac{2}{(R^*)^2}. \tag{40}$$

If $R > R^*$, then $V_1(R) > 0$, therefore the wave moves along the positive direction of the $x$ axis, and if $R < R^*$ then vice versa.

Fig.6 shows the dependence of the expansion velocity $w_{xout}$, of the phonon pulse, on the initial relative velocity $w_0$, calculated from Eqs. (36) and (35). We see that for strongly anisotropic phonon systems, when $w_0 \sim c$, the

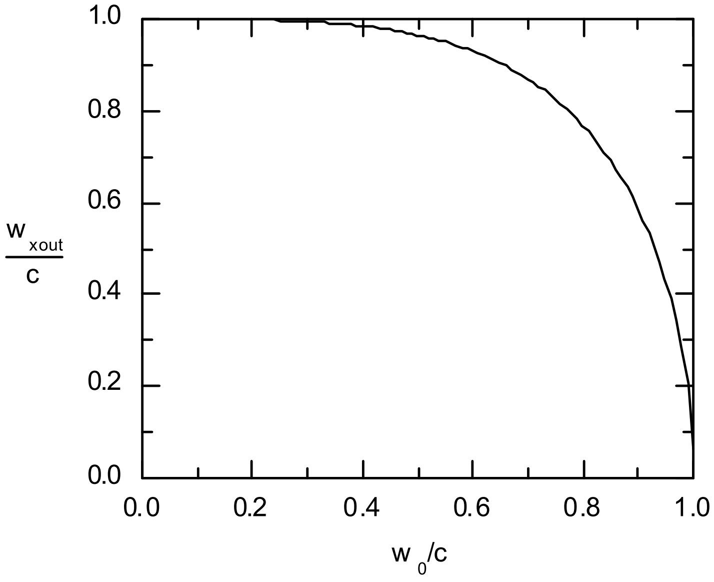

Figure 6: The dependence of the expansion velocity $w_{xout}$ of the phonon pulse on the initial relative velocity $w_0$.

expansion velocity $w_{xout}$ can be very small, compared to the phonon velocity. When $w_0 \ll c$, then $w_{xout} \sim c$, and phonon system expands nearly with the phonon velocity.

The self-similar solution Eqs. (33), (34), (23), (32), and (27), together with the unaffected region which remains constant , determine the desired solution of the initial value problem for Eqs. (9), (10), and (30) everywhere only till moment of time $t_0$. At this moment of time the front of the ingoing wave, which propagates in the region $x > 0$, reaches the coordinate origin $x = 0$, and meets the front of the ingoing wave which propagates in the region $x < 0$ in a symmetric way to the $x > 0$ wave. At $t > t_0$ these two waves overlap at the centre region of the phonon pulse. Thus a reflected wave arises in the region $0 < x < x_{ref}(t)$, when $t > t_0$. In the region $x_{ref}(t) < x < x_{out}(t)$ the solution remains self-similar, and is described by the same formulae (33), (34), (23), (32), and (27). The point $x_{ref}(t)$ is determined from the condition of a continuous join between the reflected wave and the self-similar solution.

Because we cannot find the analytical solution for the reflected wave, we consider in the next section the approximate method for its description.

# 5 Approximate description of the reflected wave

At the time $t = t_0$, when the front of the ingoing wave reaches the coordinate origin $x = 0$, the $x$-coordinate derivative of the energy density has a maximum at $x = 0$, and the initial plateau on the energy density curve has shrunk to zero. After the time $t = t_0$, when the reflected wave appears, it transfers the energy from the coordinate origin, where the energy density is maximal, to the periphery, where the energy density tends to zero. As a result, in the region $0 < x < x_{ref}(t)$ the energy density curve has an approximate plateau, where the $x$-coordinate derivative of the energy density is small compared to the one in the region where the reflected wave has not reached. This dependence of the energy density on the $x$-coordinate (or on the angle between the normal to the heater and the detector) has been experimentally studied recently in Ref. [5]. At the present time we cannot find the analytical solution for the reflected wave because there are no general methods for solving nonlinear equations of the form (9) and (10). However preliminary numerical calculations confirm the picture presented here.

Starting from the condition that the reflected wave and the incident wave join continuously, and using the energy conservation law, we can find approximately the average energy density and the average width of the reflected wave. For this purpose let us formulate the energy conservation law for one dimensional phonon propagation in superfluid helium.

For a phonon system with a linear energy-momentum relation $\varepsilon = cp$, it is easy to obtain the energy density

$$E = \frac{\pi^2}{30} \frac{k_B^4 T^4 (1 + w^2/(3c^2))}{\hbar^3 c^3 (1 - w^2/c^2)^3}. \tag{41}$$

The energy conservation law can be written as

$$\frac{\partial E}{\partial t} + \frac{\partial Q_E}{\partial x} = 0, \tag{42}$$

where $Q_E$ is the phonon energy density flux in the $x$-direction

$$Q_E = \frac{2\pi^2}{45} \frac{k_B^4 T^4 w_x}{\hbar^3 c^3 (1 - w^2/c^2)^3}. \tag{43}$$

The energy conservation law (42) along with the expression for the energy density flux (43) can be derived directly from the system of equations (9) and (10), which describe the propagation of the phonon system in superfluid helium.

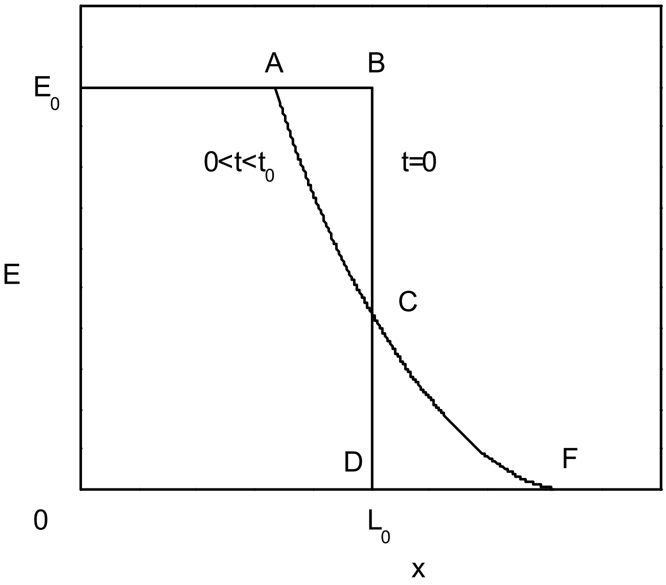

Figure 7: The solid line $ACF$ presents the spatial dependence of the phonon energy density $E$ at some time $0 < t < t_0$.

When the phonon expansion is described by (9) and (10), together with the initial conditions (30), the total energy, which is localized at the half-plane $x > 0$, does not depend on time due to the energy conservation law (42) and the symmetry of the initial conditions (30). This energy is equal to $E_0 L_0$, where $E_0 = E(T_0, w_0) = E(R_0)$ is the initial phonon energy density (41).

On Fig.7 the solid line represents the spatial dependence of the phonon energy density (41) at some time $0 < t < t_0$, while the phonon pulse expansion is described by the self-similar solution (33), (34), (23), (32), and (27) (line $ACF$). The energy conservation law leads to the equality of areas $ABC$ and $CDF$ in Fig.7.

At the time $t > t_0$, in the central region $0 < x < x_{ref}(t)$, there is a reflected wave. In the region $x > x_{ref}(t)$ the solution is the self-similar wave. To find approximately the average energy density and the average width of the reflected wave we formally continue this self-similar solution into the region $x < x_{ref}(t)$ until some point $x_m(t)$, which is characterised by the energy density $E_m(t)$. We show this in Fig.8, where the self-similar wave is drawn at some time $t > t_0$. This value $E_m(t)$ along with $x_m(t)$ is determined from the condition that the shaded area on Fig.8 is equal to the initial energy

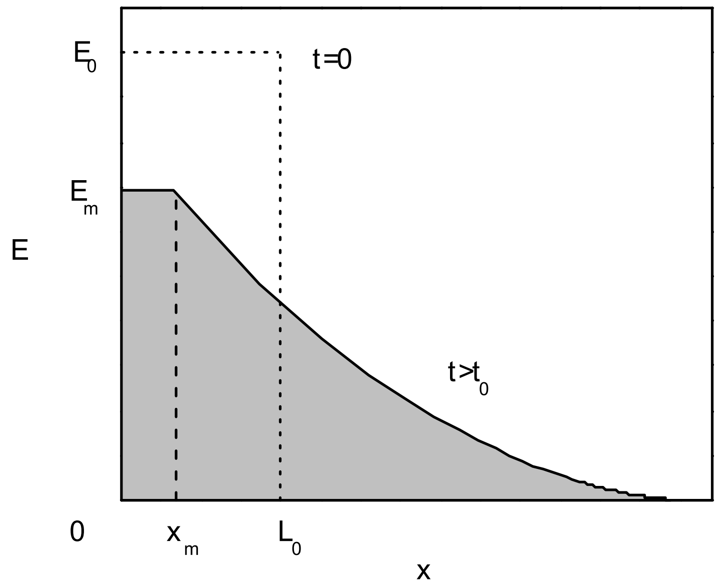

Figure 8: The solid line presents the spatial dependence of the phonon energy density $E$ at some time $t > t_0$. The values $x_m$ and $E_m$ shows the approximate position and the average energy density in the reflected wave respectively.

$E_0 L_0$. Thus we can write the equation for $E_m$ and $x_m$

$$E_m x_m + \int_{R_m}^{+\infty} E(R) \frac{\partial x(R)}{\partial R} dR = E_0 L_0, \tag{44}$$

where $x_m = x(R_m)$ (see Eq. (32)) and $E_m = E(R_m)$.

Substituting in Eq. (44) the expression (32) for $x$-coordinate, we get after integration by parts

$$t_m = \frac{(E(R_m) - E_0) L_0}{\int_{R_m}^{+\infty} V_1(R) \frac{\partial E(R)}{\partial R} dR}. \tag{45}$$

The expression (45) determines approximately the time $t_m$, when the reflected wave reaches the value $R_m > R_0$. Note that the integral in the denominator of Eq. (45) tends to zero at $R_m = R_0$. This is a mathematical expression of the equality of areas $ABC$ and $CDF$ in Fig.7 at any time $t < t_0$.

It should be noted that if the energy density gradient was zero in the reflected wave region, then we would have the equality $x_m(t) = x_{ref}(t)$ and Fig.8 would show the exact spatial dependence of the energy density, with the characteristic plateau in the central region. As it is clear from a physical point

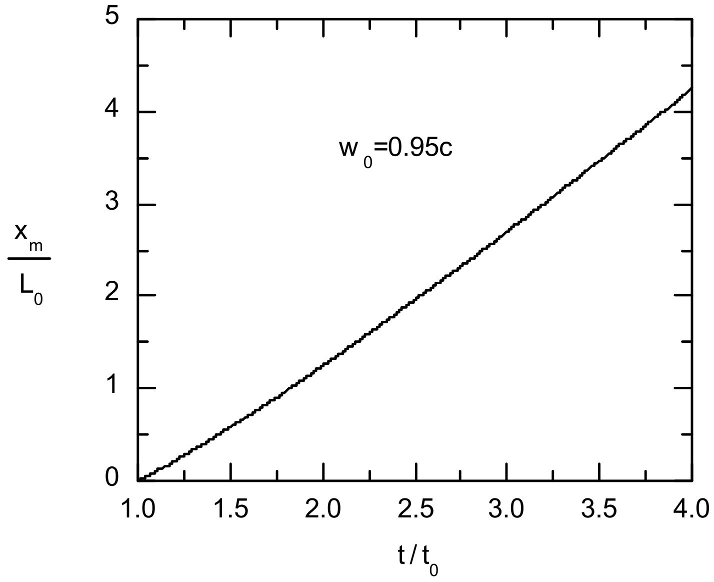

Figure 9: The dependence of the approximate width $x_m$ of the reflected wave on time $t$ for the initial value of $w_0 = 0.95c$.

of view and preliminary numerical calculations, in the reflected wave region, the energy density gradient is much smaller than the one in the ingoing wave, but not equal to zero. Therefore $x_m(t)$ does not coincide with $x_{ref}(t)$. In fact, because $dE/dx < 0$, $x_m(t) < x_{ref}(t)$. But the difference between $x_m(t)$ and $x_{ref}(t)$ is small, if the energy density gradient is small in the reflected wave region compared to the one in the ingoing wave. So the theory, developed above, allows us to find the average energy density and the average width of the reflected wave. This width corresponds to the width of the mesa shape in the angular distributions observed in [5].

Fig.9 shows the dependence of the approximate width $x_m$ of the reflected wave on time $t$, calculated from Eqs. (45), (32), (41), (33), (34), (23) and (27). In Fig.9 we see that this dependence is nearly linear. This corresponds to the constant velocity of the front of the outgoing self-similar wave. In the experiments [5] it was found that the mesa width increased with the distance from the heater which is the same as the dependence of $x_m$ on time in Fig.9.

The average energy density in the reflected wave $E_m$ as a function of time $t$ is presented in Fig.10. It is calculated from Eqs. (45), (41), (33), (34), (23), and (27). We see that the approximate average energy density in the reflected wave $E_m$ decreases monotonically with time because of the expansion of the phonon pulse. The dependence of $E_m$ on time (Fig.10) is

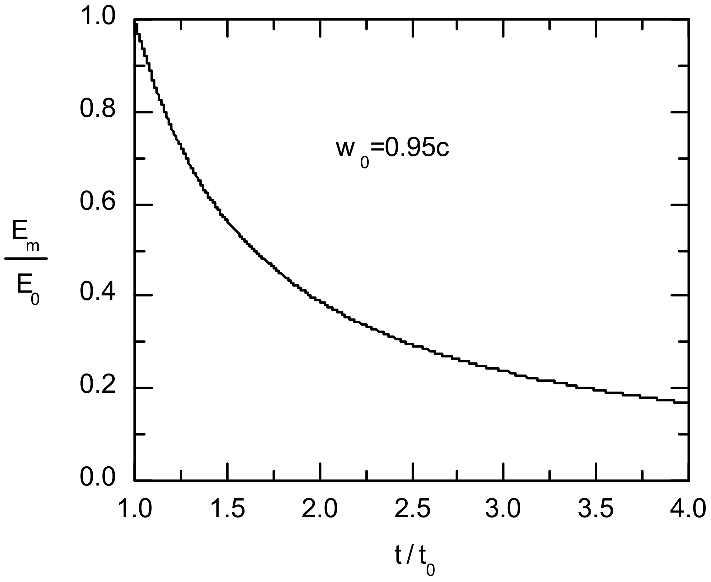

Figure 10: The dependence of the approximate average energy density $E_m$, of the reflected wave, on time $t$ for the initial value of $w_0 = 0.95c$.

similar to that observed in experiments [5] where the mesa height decreased with the distance from the heater.

# 6 Comparison with the experimental data

Initially, the phonon pulse created by the heater (see Fig.1), is comprised of low energy phonons (l-phonons), which immediately start to create high energy phonons (h-phonons) [18]. The h-phonon creation results in spatially smoothing the initial hot nonuniform central region of l-phonon pulse, which is injected by heater into superfluid helium. However the h-phonon creation for short pulses occurs mainly near the heater within a distance of several millimeters [18]. The h-phonon creation time can be roughly estimated as 10 $\mu$s for the typical experimental heater powers. This time corresponds to the phonon travelling a distance 2.4 mm. The initial conditions (30) for the l-phonon system correspond to the end of the h-phonon creation stage of the evolution of the phonon system. So the above theory is for the expansion of a cool l-phonon system.

After the h-phonon creation rate has become negligible, the temperature is $T_0$ and the relative velocity is $w_0$. The values of $T_0$ and $w_0$ depend on the power applied to the heater. Their values for l-phonon pulses, with a linear

| Power | Initial values | |
|---|---|---|
| $P$, mW | $T_0$, K | $w_0/c$ |
| 3.125 | 0.033 | 0.955 |
| 6.25 | 0.041 | 0.947 |
| 12.5 | 0.050 | 0.938 |
| 25 | 0.065 | 0.921 |

Table 1: The values of temperature $T_0$ and the relative velocity $w_0$ (divided by first sound velocity $c = 238$ m/s) for the l-phonon system with different values of the heater power P.

momentum-energy relation, are calculated using the results of [18] for experimentally applied powers. The results of these calculations are presented in Table 1 for the heater powers used in the experiments [5]. The second and third columns show the corresponding values of temperature $T_0$ and the relative velocity $w_0$ for these powers. Using the theory presented in this paper, we can find at any time the spatial dependencies of all the parameters of the l-phonon system for different powers, which correspond to the values of $T_0$ and $w_0$ in Table 1.

We should note that the phonon pulses created in experiments [5] are not long enough to neglect the $z$-coordinate dependence in the phonon evolution system (5), (6). Moreover the experimental conditions are much more close to cylindrical symmetry, then to a plane one. Nevertheless we think that the qualitative dependencies, obtained here for a plane phonon layer, can be compared to the real much more complicated experimental conditions.

The theory presented here shows that the initial phonon pulse starts to expand into the "phonon vacuum". The simple second sound wave appears with the outgoing wave front moving into the "phonon vacuum", and the front of the ingoing wave moving to the centre at $x = 0$ (see Fig.3). During this time, the width of initial plateau decreases with time. So at the time $t_0$ (see Eq. (31)) there is no mesa. The phonon pulse propagates a distance of $l_0 = ct_0$ during this time. For the initial pulse width $2L_0 = 1$ mm and for powers 3.125 mW, 6.25 mW, 12.5 mW, and 25 mW from Ref. [5], we obtain the values of $l_0$ of 2.4 mm, 2.3 mm, 2.1 mm, and 1.9 mm respectively. The total distance between the heater and the phonon pulse $l_h$ is $l_h = l_0 + l_c$, where $l_c = 2.4$ mm is the length after which the h-phonon creation has effectively stopped. Note that this schema of taking into account of h-phonon creation is rather rough one, especially for high powers.

In experiments [5] the minimal distance between heater and detector was

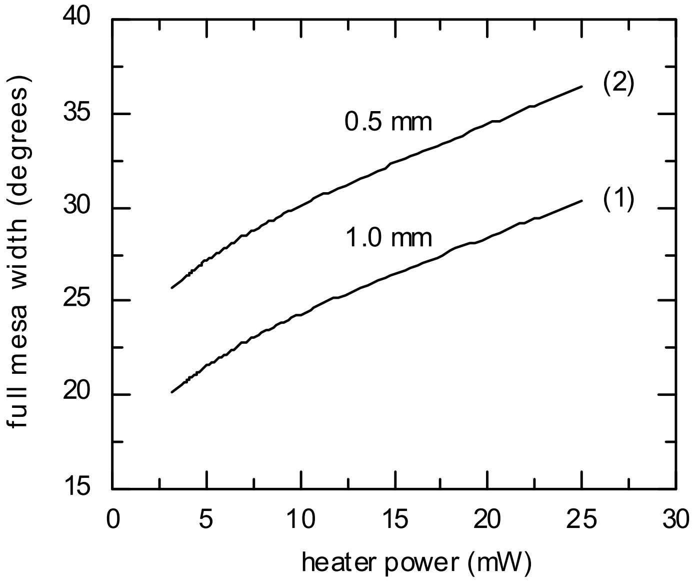

Figure 11: The dependencies of the full mesa width $2x_m$ in degrees, on heater power for the distance 12.3 mm from the heater, for the heater widths $2L_0 = 1$ mm (line 1) and for $2L_0 = 0.5$ mm (line 2).

8.2 mm. Thus the decrease in the width of the initial plateau is not observed in [5]. It would need measurements of the phonon energy angular distributions at a distance about 3-4 mm from the heater to compare with this prediction of the theory that there is no mesa at $\approx 4$ mm.

At time $t = t_0$ the reflected wave appears. From a physical point of view it is clear that in the reflected wave, which occurs in the central region of the phonon pulse, the energy density gradient is smaller than in the ingoing wave. Thus the existence of the reflected wave should lead to a mesa shape in the phonon angular distributions at distances larger than $\approx 4$ mm.

In Ref.[5] the detailed measurements of l-phonon angular distributions in superfluid helium showed a distinct mesa shape. The dependence of the mesa height and width, on heater dimensions, distance to the detector and heater power, were measured [5]. Using the theory presented in this paper we now can give qualitative explanations some of these experimental data.

In Fig.11 we show the dependencies of mesa width $x_m$ on power for the distance 12.3 mm from the heater for the heater widths $2L_0 = 1$ mm (line 1) and for $2L_0 = 0.5$ mm (line 2), calculated from the data in Table 1 and Eqs. (45), (32), (33), (27), (35) and(23). Here and below we take the distances and the heater widths which were used in the experiments [5]. We see the

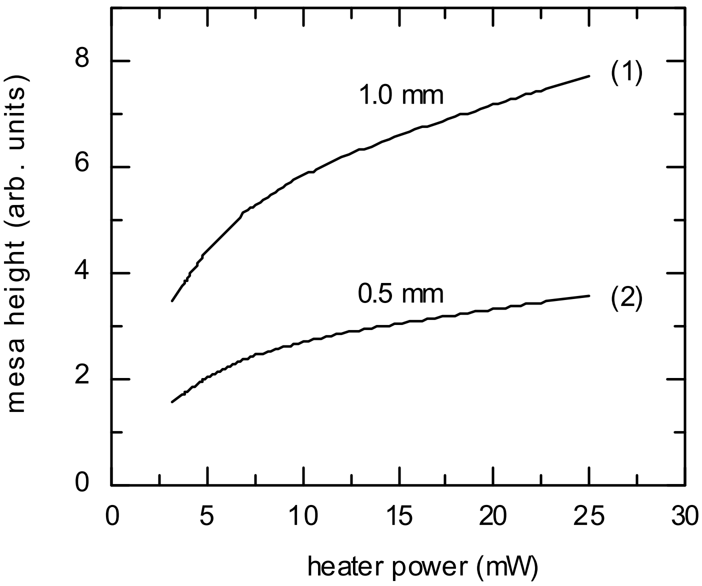

Figure 12: The dependencies of the mesa height $E_m$ on power for the distance 12.3 mm from the heater for the heater widths $2L_0 = 1$ mm (line 1) and for $2L_0 = 0.5$ mm (line 2).

monotonic growth of the mesa width $x_m$, when power increases as it does in the experimental data from [5], although the measured mesa widths are considerably smaller than those theoretically predicted. The power dependence can be explained in the following way. When power increases, the relative velocities $w_0$ decrease (Table 1). This results in increasing the absolute value of velocity $V_1$. Thus the time $t_0$ (see Eq. (31)) decreases, and the mesa forms earlier. It should be noted that in the experiments [5] for some cases the measured mesa widths start to decrease at high power 25 mW (see Fig. 9 of [5]). Our theory, which describes the expansion of a cool l-phonon layer, cannot explain this effect.

In Fig.12 we present the dependencies of the mesa height $E_m$ on power for the distance 12.3 mm from the heater for the heater widths $2L_0 = 1$ mm (line 1) and for $2L_0 = 0.5$ mm (line 2), calculated from the data in Table 1 and Eqs. (45), (33), (34), (27), (35) and(23). The mesa height $E_m$ increases, when the power increases, as it does in the measured data [5].

While the mesa width $x_m$ do not depend on the initial temperature $T_0$, which follows from Eqs. (45) and (32), the mesa height $E_m$ depends on $T_0^4$. It turns out that the increase of $T_0$ with power prevails over the decrease the relative velocity $w_0$, and so an increase in power leads to a quicker expansion

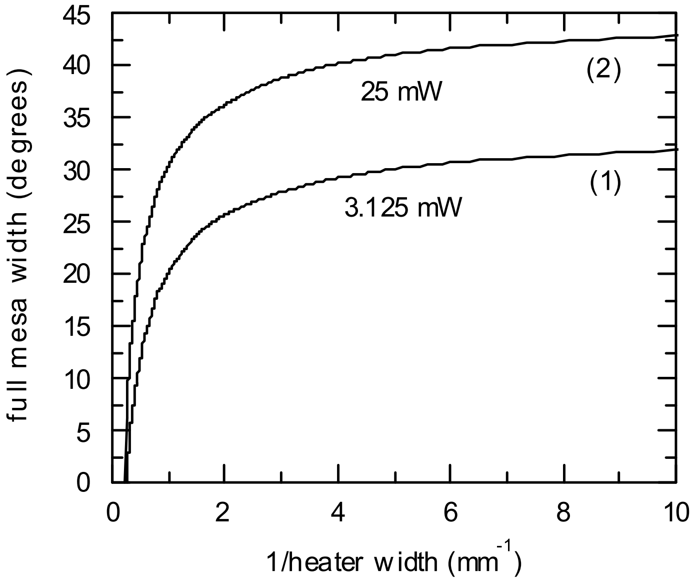

Figure 13: The angular width of the full mesa $2x_m$ versus the inverse of the heater width for the distance 12.3 mm from the heater, for heater powers 3.125 mW (line 1) and 25 mW (line 2).

of the phonon pulse and hence to a wider mesa.

The increase of $x_m$ with time, shown in Fig.9 corresponds to an increase of the mesa width with distance. This is observed in experiments [5]. The decrease of $E_m$ with time, shown in Fig.10, corresponds to a decrease in the mesa height with distance. This too is observed in experiments [5].

The theory developed in this paper allows us to qualitatively understand why the mesa width increases with decreasing the heater width [5]. A smaller heater width ($2L_0$) results in an earlier formation of the mesa, and this leads directly to an increase in the mesa width. In Fig.13 we show the dependencies of mesa width $x_m$ on reciprocal heater width $1/(2L_0)$ for the distance 12.3 mm from the heater for powers 3.125 mW (line 1) and 25 mW (line 2), calculated from the data in Table 1 and Eqs. (45), (32), (33), (27), (35) and (23). But we should note that our theory does not reproduce the linear dependence of mesa width on reciprocal heater width, which was observed in the experiments [5] (see Fig. 10 in [5]).

# 7 Conclusions

In this paper, starting from the hydrodynamic equations of superfluid helium, we have obtained the system of equations (5) and (6), which describe the evolution of a cool phonon systems, created by thermal pulses in superfluid helium for the case $\rho_n \ll \rho$ (see Fig.1). These equations are simplified to the case of one spatial dimension (see Eqs. (8)-(10), and Fig.2). The family of exact solutions were found in an explicit analytical form. They are the simple waves of second sound for phonon systems. The relations between temperature $T$ (26), the $x$-component $w_x$ (22) of the relative velocity $\mathbf{w}$, and the square of the relative velocity $w^2$ (23) are studied for the simple second sound waves in phonon systems. These solutions are used to describe the first stage of expansion of a phonon layer in superfluid helium, when only simple second sound waves exist. Figs.3, 4, and 5 show the spatial dependence of temperature $T$ (Fig.3), the $x$-component $w_x$ (Fig.4) of the relative velocity $\mathbf{w}$, and the square of the relative velocity $w^2$ (Fig.5) for time $t = 0$ (dashed lines on Figs.3 and 5), $t = t_0/2$ (dotted lines in Figs.3, 4, and 5), and for $t = t_0$ (solid lines in Figs.3, 4, and 5).

We have found the velocity of expansion $w_{xout}$ of a phonon pulse, propagating initially in $z$-direction, into the "phonon vacuum", i.e. into superfluid helium at zero temperature. The dependence of the expansion velocity $w_{xout}$ of the phonon pulse, on the initial relative velocity $w_0$, calculated from Eqs. (36) and (35) are presented in Fig.6. We see that for strongly anisotropic phonon systems, when $w_0 \sim c$, the expansion velocity $w_{xout}$ can be small compared to the phonon velocity. When $w_0 \ll c$, then $w_{xout} \sim c$, and phonon system expands nearly with the phonon velocity.

In the second stage, after the incident wave reaches the centre of the phonon layer, a reflected wave appears. We found the time $t_0$ Eq. (31), when this starts. The reflected wave transfers energy from the coordinate origin, where the energy density is maximal, to the periphery, where the energy density tends to zero. It smooths the dependence of the energy density on the $x$-coordinate, in the reflected wave region. The smallness of the $x$-coordinate derivative of the energy density in the reflected wave region, compared with the one in the ingoing wave, results in a mesa shape form, which was observed in [5].

We developed an approximate theory for the average energy density and the average width of the reflected wave (see Fig.8). The calculated dependencies of the mesa height and mesa width on time (Figs.9, 10), on the heater power (Figs.11, 12), and on the heater width (Fig.13) show partly the same qualitative dependencies as the experimental data in [5], although our theory fails to explain all effects observed. But we think that the main cause of the mesa shape appearance in the experiments [5] are the same as in our simple model theory.

# Acknowledgements

We thank very much A. F.G. Wyatt for drawing our attention to this problem and for many useful discussions, and we express our gratitude to EPSRC of the UK (grant EP/F 019157/1) for support of this work.

# References

[1] A. F. G. Wyatt, N. A. Lockerbie and R. A. Sherlock, *Phys. Rev. Lett.*, **33**, 1425 (1974).

[2] R. Vovk, C.D.H. Williams, and A.F.G. Wyatt, *Phys. Rev. Lett.*, **91**, 235302 (2003).

[3] D.H.S. Smith, R.V. Vovk, C.D.H. Williams and A.F.G. Wyatt, *New Journal of Physics* **8**, 128 (2006).

[4] D.H.S. Smith and A.F.G. Wyatt, *Phys. Rev. B*, **76**, 224519 (2007).

[5] D.H.S. Smith and A.F.G. Wyatt, *Phys. Rev. B*, **79**, 144520 (2009).

[6] I.N. Adamenko, Yu.A. Kitsenko, K.E. Nemchenko, V.A. Slipko and A.F.G. Wyatt, *Low Temp. Phys.*, **31**, 459 (2005).

[7] D.H.S. Smith, R.V. Vovk, C.D.H. Williams, and A.F.G. Wyatt, *Phys. Rev. B*, **72**, 054506, (2005).

[8] A.F. Andreev and L.A. Melnikovsky, *J. of Low. Temp. Phys.*, **135**, 411(2004).

[9] I.N. Adamenko, K.E. Nemchenko, V. A. Slipko, and A.F.G. Wyatt, *Phys. Rev. B*, **68**, 134507, (2003).

[10] I.N. Adamenko, K.E. Nemchenko, V.A. Slipko and A.F.G. Wyatt, *J. Low Temp. Phys.*, **138**, 67 (2005).

[11] I.N. Adamenko, K.E. Nemchenko, V.A. Slipko and A.F.G. Wyatt, *J. Phys.: Condens. Matter*, **17**, 2859 (2005).

[12] I.M. Khalatnikov, *An Introduction to the Theory of Superfluidity*, W.A. Benjamin, New York - Amsterdam, 1965.

[13] S.J. Putterman, *Superfluid Hydrodynamics*, North Holland, Amsterdam, 1974.

[14] I.N. Adamenko, K.E. Nemchenko, V.A. Slipko and A.F.G. Wyatt, *Phys. Rev. B*, **79**, 104508, (2009).

[15] I.N. Adamenko, K.E. Nemchenko, V.A. Slipko and A.F.G. Wyatt, *J. Phys.: Condens. Matter.* **18**, 2805 (2006).

[16] L.D. Landau, E.M. Lifshitz, *Fluid Mechanics*, Oxford, Pergamon Press, 1987.

[17] I.N. Adamenko, K.E. Nemchenko, V.A. Slipko and A.F.G. Wyatt, *Phys. Rev. B*, **77**, 144515, (2008).

[18] I.N. Adamenko, Yu.A. Kitsenko, K.E. Nemchenko, V.A. Slipko and A.F.G. Wyatt, *Phys. Rev. B*, **73**, 134505, (2006).